Liquid Crystals
Publication details, including instructions for authors and subscription information:
http://www.informaworld.com/smpp/title~content=t713926090

Controlling the orientation of microgrooves and the depth of the ripple structure in dye-doped liquid crystal cells

I. Palarie[a]; C. Dascalu[b]; G. E. Iacobescu[a]
[a] Faculty of Physics, University of Craiova, Craiova, Romania [b] Physics Department, Faculty of Applied Physics, University Politehnica of Bucharest, Bucharest, Romania

Online publication date: 11 February 2010

To cite this Article Palarie, I. , Dascalu, C. and Iacobescu, G. E.(2010) 'Controlling the orientation of microgrooves and the depth of the ripple structure in dye-doped liquid crystal cells', Liquid Crystals, 37: 2, 195 — 199
To link to this Article: DOI: 10.1080/02678290903484222
URL: http://dx.doi.org/10.1080/02678290903484222

Liquid Crystals,
Vol. 37, No. 2, February 2010, 195–199

Taylor & Francis
Taylor & Francis Group

Controlling the orientation of microgrooves and the depth of the ripple structure in dye-doped liquid crystal cells

I. Palarie[a], C. Dascalu[b]* and G.E. Iacobescu[a]

[a]*Faculty of Physics, University of Craiova, Craiova, Romania;* [b]*Physics Department, Faculty of Applied Physics, University Politehnica of Bucharest, Bucharest, Romania*

(Received 1 October 2009; final version received 12 November 2009)

The permanent structure induced by an Ar^+ linearly polarised laser beam on an asymmetric dye-doped nematic liquid crystal cell was investigated in a pump-probe experiment. The polarisation direction of the probe beam was parallel to the easy axis and two configurations of pump beam were used: polarisation directions perpendicular and parallel to the easy axis. The transmitted intensity of the probe beam was recorded during irradiation and it was observed that it depended both on the power and polarisation direction of the pump beam. We explained the evolution of the transmitted intensity and evaluated the start time of formation of the ripple structure. The induced permanent structure in the irradiated zones and the laser-induced surface morphology was studied using a polarising optical microscope and an atomic force microscope, respectively. The surface morphology in the irradiated zones was also dependent on both the power and polarisation of the Ar^+ laser beam. The orientation of the microgrooves in the ripple structure was parallel to the polarisation direction of the pump laser beam in both configurations. For a given pump power, the depth of the ripple structure was greater in the case of an Ar^+ beam polarised parallel to the easy axis. The induced azimuthal anchoring energy provided by the ripple structure was evaluated.

Keywords: nematic liquid crystal; azo dye; ripple structure; atomic force microscopy

1. Introduction

The photo-alignment effect in dye-doped liquid crystal (DDLC) films induced by a laser beam has become important in recent years because of its potential applications in the LC display industry. If the alignment of LCs is performed by rubbing a polyimide/polymer film coated on glass plates problems can result due to static electricity, dust particles and other residues on the rubbed surface. These problems may be avoided by using the photo-alignment method [1]. Photo-alignment can be achieved by doping azo dyes into LCs. Lucchetti *et al.* [2] and Fuh *et al.* [3] observed the dye-induced LC reorientation on the surface with and without polymer coating, respectively. Under proper irradiation with blue-green light, methyl-red (MR) molecules tend to be adsorbed on to the surface of the substrate, reorienting the LC molecules into a new permanent configuration [4]. The surface morphology of the adsorbed substrate has been studied by Lee *et al.* [5] and three different morphologies were observed: a homogeneous and fine layer of adsorbed dyes; a layer with microgrooves; an inhomogeneous ribbon-like and rough adsorbed layer. The first and second types of layer dominate in the early and late stages, respectively, in a weak-intensity regime, tending to reorientate the LC perpendicular and parallel to the polarisation direction of the pump beam. The last type of layer dominates in a strong-intensity regime, possibly severely disturbing the orientation of the LC.

The biphotonic laser-induced ripple structure on DDLC films has been studied by Fuh *et al.* [6]. In a recent paper, Huang *et al.* [7] reported on the dynamics of photo-alignment in azo dye-doped LCs.

The aim of our study was to investigate the photo-alignment effect induced by an Ar^+ linearly polarised laser beam on a sandwich glass cell filled with 4′-n-pentyl-4-cyanobiphenyl (5CB) doped with MR in a pump-probe experiment. The polarisation direction of the He-Ne probe beam was parallel to the easy axis induced by rubbing one of the two polymeric films coated on to the glass plates. The photo-alignment effect of the pump Ar^+ laser beam was studied for various powers of the pump laser and for polarisation direction of the pump beam parallel and perpendicular to the easy axis. The evolution of the transmitted intensity of the probe beam during irradiation was explained taking into account the photo-alignment effect and the dichroism of the MR molecules. The images of the sample in the pumped areas obtained by using a polarising optical microscope (POM) confirmed the results of the pump-probe experiment. The irradiated zones were studied by atomic force microscopy (AFM) and the surface

*Corresponding author. Email: dascaluc@yahoo.com

ISSN 0267-8292 print/ISSN 1366-5855 online

DOI: 10.1080/02678290903484222
http://www.informaworld.com

morphology depended on the power and polarisation direction of the Ar^+ laser beam. The spacing and depth of the laser-induced ripple structure were also measured and the azimuthal anchoring energy was evaluated.

2. Experimental procedure

The measurements were carried out at a temperature of 25°C using a standard sandwich glass cell filled with a mixture of a nematic LC 5CB and azo dye MR as a dopant (dye concentration was 1.5% wt).

The thickness of the cell was 23 μm (obtained by using Mylar spacers). The inner surface of the glass plates were previously covered with a thin polymeric film using a spin-coating method. The monomer, polyvinyl alcohol (PVA), was dissolved in water at a concentration of 1.5% wt. The PVA solution was spin-coated on to the glass plates, baked at 120°C for 60 min and then cooled at room temperature. An easy axis was induced by rubbing one surface in a unique direction. This orientated surface (or reference surface, S_R) imposed the planar orientation of the nematic director for the whole cell in the initial state. The other surface (command surface, S_C) is quasi-isotropic and in our experiments the exciting laser beam impinged through it. The optical arrangement used for the pump-probe experiment is schematically shown in Figure 1. This new experimental set-up was an improved version of that used in Voloshchenko *et al.* [8]. The cell was placed normal to the exciting beam of the Ar^+ laser ($\lambda = 476.5$ nm; power P_{exc} was varied between 5 and 30 mW; the irradiation time was fixed at 9 min). The irradiation time was very short compared with that used by Lee *et al.* [5] (i.e. 3 h). The diameter of the Ar^+ laser spot on the cell was about 2 mm and the mean intensity of the pump beam in the irradiated areas was between 160 and 960 mW cm^{-2} (corresponding to 5 and 30 mW, respectively), which are typical for a strong-intensity regime. The direction of rubbing on S_R was along the vertical axis. The measurements were carried out for two configurations: an Ar^+ laser beam polarised vertically and horizontally. The polarisation direction of the beam emerging from the Ar^+ laser was vertical and in the case of irradiation of the cell with a beam that must be polarised vertically, the half-wave plate ($\lambda/2$) was excluded from the experimental set-up and the polariser P_2 had a vertical transmission direction.

The other configuration was obtained by using the half-wave plate placed such that one of the neutral lines made an 45° angle with the vertical direction and the polariser P_2 with a horizontal transmission direction.

The polarisation direction of the He-Ne laser beam was established by the polariser P_1, which had a vertical transmission direction (parallel to the easy axis of the sample). The spot of the probe beam ($\lambda = 633$ nm, power P_{probe} around 1 mW) was covered by that of the pump light. After passing through the cell, the probe beam was deviated by a beam-splitter and went through the analyser, the transmission direction of which was horizontal. The probe beam intensity measurement was performed by an optical fibre connected to a S2000 spectrometer (Ocean Optics Dunedin, FL, USA) and a computer. The intensity of the transmitted probe beam was recorded during irradiation of the cell, in different zones, at different powers of the pump (i.e. 5, 12, 25 and 30 mW). After irradiation, the induced permanent structure in the sample was studied using a POM. In order to study the laser-induced surface morphology, the sample was submerged in a solvent, hexane, for a few minutes until the 5CB dissolved. The glass plate of the cell with the S_R was transparent and this demonstrated that the MR molecules had not been adsorbed on to this surface. On the other glass plate, red zones appeared which coincided with the pumped regions. These red zones are MR molecules adsorbed on to the S_C during irradiation of the sample. The morphology of the pumped regions on the S_C was analysed by using an AFM.

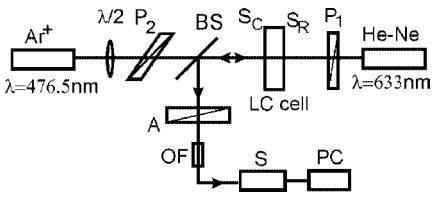

Figure 1. The experimental set-up. A: analyser; BS: beam-splitter; OF: optical fibre; PC: computer; S: spectrometer.

3. Results and discussion

The intensity of the transmitted probe beam as a function of the irradiation time for different powers of the horizontally polarised pump laser is presented in Figure 2. it was noticed that the transmitted intensity begins to increase after an irradiation time, t_{bh}. It was found that t_{bh} decreases if the power increases, the values of t_{bh} being 65, 43 and 35 s for $P_{exc} = 5$, 12 and 25 mW, respectively. The transmitted intensity can increase during irradiation if an easy axis is induced on the S_C and the angle between this gliding induced easy axis and the vertical direction also increases. The ripple orientation is parallel to the polarisation direction of the pump beam [5], and consequently, a twisted nematic structure is generated in the pumped region.

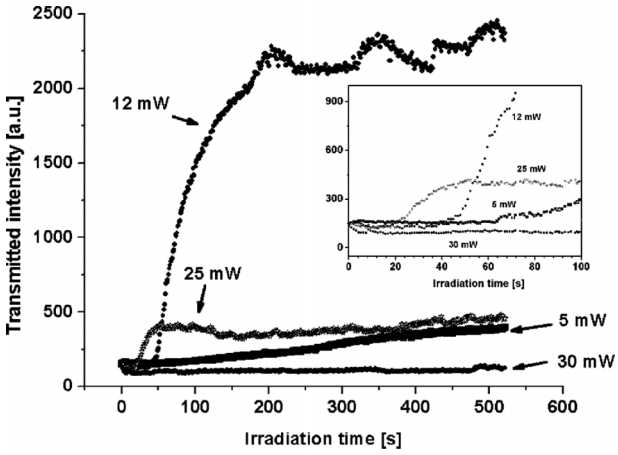

Figure 2. Transmitted intensity versus irradiation time for an Ar^+ pump laser polarised horizontally.

The time t_{bh} corresponds to the start time of formation of the ripple structure. For $P_{exc} = 12$ mW, the transmitted intensity is greater than that for 5 mW due to the fact that the ripple structure grows more quickly at a higher intensity of the pump laser beam. At 25 mW, the recorded intensity is less than that for 12 mW because at higher power the concentration of MR molecules in the cis-isomer form increases and the absorbance of MR in the red light region also significantly increases [9]. For 30 mW, the cis-isomer concentration increases quickly and the probability that the dye aggregates significantly increases. These aggregates are adsorbed on to microgrooves to form ribbon-like adsorbents and have a poor capacity for aligning LC molecules in the direction parallel to the polarisation direction of the pump beam.

The transmitted intensity of the probe beam in the case of the Ar^+ laser beam polarized vertically is shown in Figure 3. By comparing Figure 2 with Figure 3, it can be deduced that the evolution of the

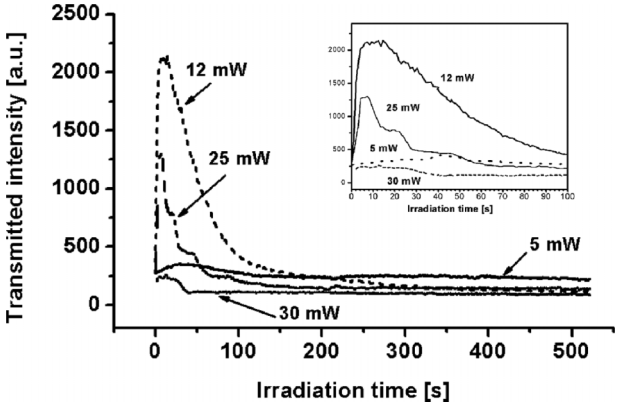

Figure 3. Transmitted intensity versus irradiation time for an Ar^+ laser beam polarised vertically.

recorded signal depends on the polarisation of the pump beam. For a pump beam polarised vertically, the transmitted intensity increases quickly and begins to decrease after an irradiation time t_{bv}. At the beginning of the irradiation the transmitted intensity increases because of the homogeneous and fine layer of adsorbed dye molecules that induce a horizontal easy axis on the S_C.

For an Ar^+ beam polarised vertically, the orientation of the ripple structure is vertical and the transmitted intensity begins to decrease when generation of the ripple structure is initiated. The values of t_{bv} are 40, 14 and 7 s for P_{exc} equal to 5, 12 and 25 mW, respectively.

The relative evolution of the transmitted probe beam for different pump powers in the case of an Ar^+ beam polarised vertically can be explained in a similar manner for that of horizontal polarisation. For a given power of the pump beam, $t_{bv} < t_{bh}$. This result can be explained because MR is an azo dye with a dichroic ratio, D, defined as $A_{II}/A_{\perp}$, of approximately six for visible light [6]. A_{II} and $A_{\perp}$ are the dye absorbancies when the polarisation of the pump beam is parallel and perpendicular, respectively, to the optical axes of the dyes.

The pumped regions were investigated using a POM with crossed polarisers. The polariser was set parallel to the rubbing direction on the S_R and white light entered the cell from the S_R side. Figure 4 displays the results obtained in the case of a horizontally polarised Ar^+ beam. The pumped regions are bright while the unpumped zones are dark. As the Ar^+ laser beam is Gaussian and its intensity decreases from the centre to the periphery of the laser spot, the effect of irradiation is more pronounced in the centre of the pumped zone. The bright region demonstrates that a twisted nematic structure has been induced during irradiation. The twisted angle was measured in the centre of the zones corresponding to pump powers of 5 and 12 mW by POM as the difference between the angle of analyser direction at total extinction in the twisted sample and normal to the polariser. The obtained values were very close to 90°, which suggest that the induced ripple structure is perpendicular to the rubbing direction. For powers of 25 and 30 mW, the amount of excited dyes is believed to increase to excess in the DDLC. The trans MR molecules transform to cis-isomers and tend to aggregate when stimulated by Ar^+ light because the dipole moment of a cis-isomer is much stronger than that of a trans-isomer [5]. The absorbance of MR in the red light region increases, which implies that the cis-isomers grow rapidly and the probability that the dye aggregates with irregular orientations significantly increase.

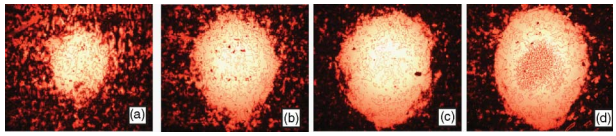

Figure 4. Images of the irradiated zones with a horizontally polarised Ar^+ laser beam obtained by using a polarising optical microscope with crossed polarisers: (a) $P_{exc} = 5$ mW; (b) $P_{exc} = 12$ mW; (c) $P_{exc} = 25$ mW; (d) $P_{exc} = 30$ mW.

For powers of 25 and 30 mW, a twisted angle cannot be measured and it was concluded that for these pump powers dye aggregates appear in the centre of irradiated zones. Such dye aggregates are visible in the centre of Figure 4(d).

The images of the zones irradiated with an Ar^+ beam polarised vertically obtained by POM with crossed polarisers are presented in Figure 5. These images are different from those corresponding to the case of a horizontally polarised Ar^+ beam. The irradiated zones are not bright because the ripple structure induced in this case is parallel to the rubbing direction, which is perpendicular to the transmission direction of the POM analyser.

Figure 5(c) and (d) present central zones with dye aggregates. By analysing the unpumped zones from Figure 5, many bright regions are observed. A possible explanation of this behaviour is the scattering of the pump beam from the dye-adsorbed surface S_C. A similar result has been reported by Huang *et al.* [7]. By comparing the unpumped zones in Figures 4 and 5, we deduced that the scattering of the Ar^+ laser beam during irradiation is greater in the case of a pump beam polarised parallel to the rubbing direction.

All the irradiated zones on the S_C were analysed by AFM. Figure 6 shows the AFM images corresponding to the central region of the irradiated zones in the case of a horizontally polarised Ar^+ beam. A ripple structure is observed for 5 and 12 mW. The orientation of the microgrooves in the ripple structure is parallel with the direction of polarisation of the Ar^+ laser beam. The mean depth of the microgrooves, A, obtained for 5 mW is around 20 nm while for 12 mW it is around 25 nm. The depth of the ripple structure increased if the pump

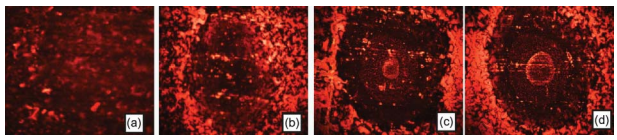

Figure 5. Images of the irradiated zones with a vertically polarised Ar^+ laser beam obtained by using a polarising optical microscope with crossed polarisers: (a) $P_{exc} = 5$ mW; (b) $P_{exc} = 12$ mW; (c) $P_{exc} = 25$ mW; (d) $P_{exc} = 30$ mW.

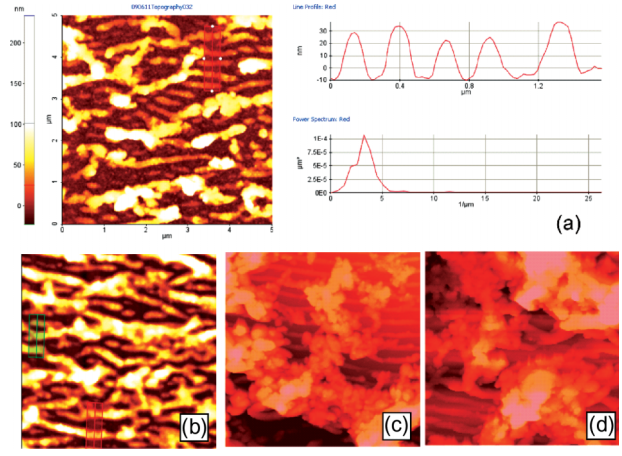

Figure 6. Atomic force microscopy images obtained for a horizontally polarised Ar^+ laser beam for various pump powers: (a) $P_{exc} = 5$ mW; (b) $P_{exc} = 12$ mW; (c) $P_{exc} = 25$ mW; (d) $P_{exc} = 30$ mW.

power was increased. The spacing between microgrooves, Λ, is around 300 nm (see Figure 6(a)).

According to the laser-induced periodic surface structure theory [10], the spacing of the resulting ripple structure in a DDLC film is given by $\Lambda = \lambda/n$, where λ is the wavelength of the pump beam in vacuum and n is the refractive index of the material adsorbed on to the surface of the DDLC cell substrate. For $\lambda = 476.5$ nm and $n \cong 1.6$ (for MR) [4], a spacing of around 298 nm was calculated, which is consistent with the experimental value. Figure 6(c) and (d) present rough and inhomogeneous surfaces obtained by rapid and random aggregation and adsorption of cis MR molecules. Important information about the roughness of the scanned area is given by the maximum 'peak-to-valley' value, R_{pv} [11]. For 25 mW, $R_{pv} = 429.84$ nm, while for 30 mW, a greater value is obtained, $R_{pv} = 863.47$ nm.

The AFM images obtained by analysing the zone irradiated with an Ar^+ laser polarised vertically are shown in Figure 7. A ripple structure was also obtained for 5 and 12 mW (see Figure 7(a) and (b)), and the microgrooves are parallel to the pump beam polarisation. The spacing is around 300 nm (as in the previous case), but the depths of the ripple structure are around 40 nm and around 60 nm for 5 and 12 mW, respectively. Figure 7(c) and (d) show the surfaces that have a higher roughness than those corresponding to the Ar^+ beam polarised horizontally. For 25 mW, $R_{pv} = 1055.00$ nm, while for 30 mW, $R_{pv} = 1276.74$ nm.

Based on Berreman's theory, the azimuthal anchoring energy provided by a grooved surface, W, is given by [12]:

$$W = 2\pi^3 A^2 K_{22}/\Lambda^3, \qquad (1)$$

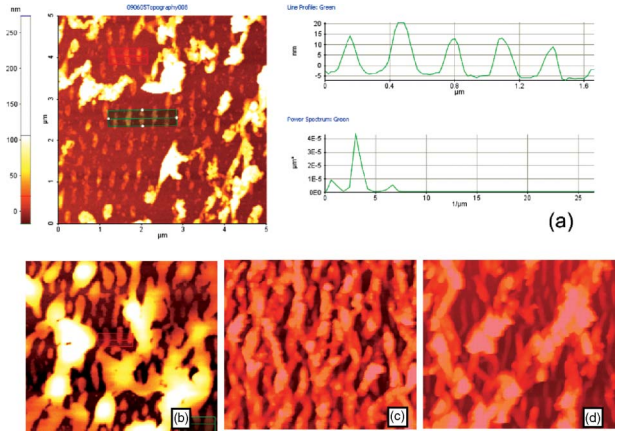

Figure 7. Atomic force microscopy images obtained for a vertically polarised Ar^+ laser beam for various pump powers: (a) $P_{exc} = 5$ mW; (b) $P_{exc} = 12$ mW; (c) $P_{exc} = 25$ mW; (d) $P_{exc} = 30$ mW.

where A and Λ are the depth and spacing of the microgroove structure, respectively, and K_{22} is the elastic constant of the LC. Substituting the obtained values for A, Λ around 300 nm, and $k_{22} = 3.9 \times 10^{-12}$N (for 5CB at 25°C [13]) into Equation (1), the azimuthal anchoring energy was evaluated.

In the case of an Ar^+ laser beam polarised horizontal, for pump powers of 5 and 12 mW, the corresponding values of W are around 0.36×10^{-5}Jm^{-2} and 0.56×10^{-5}Jm^{-2}, which are typical values for a rubbed polyimide/polimer alignment film. These values for the induced azimuthal anchoring energy are sufficient to maintain a permanent twist nematic structure in the irradiated zones.

Due to the fact that for a fixed pump power and irradiation time the depth of the ripple structure is higher in the case of an Ar^+ laser beam polarised parallel to the rubbing direction, the azimuthal anchoring energy induced by the ripple structure is also greater in this case compared with the other configuration. For an Ar^+ polarised vertically, the values of W are around 1.43×10^{-5}Jm^{-2} and 3.22×10^{-5}Jm^{-2}for pump powers of 5 and 12 mW, respectively.

4. Conclusions

In this study, the photo-alignment effect induced by an Ar^+ linearly polarised laser beam on a DDLC was investigated in a pump-probe experiment. Experimental results indicated that formation of the induced permanent structure in the irradiated zones involves bulk reorientation and surface adsorption and depends both on the power and polarisation direction of the pump beam. The role of the dichroism of MR on the obtained results was also discussed. A high scattering of the pump laser beam during irradiation was observed in the case of an Ar^+ polarised parallel to the rubbing direction.

The laser-induced surface morphology in the irradiated regions was studied by AFM. For pump powers of 25 and 30 mW, rough surfaces with inhomogeneous ribbon-like layers were obtained in both cases. A ripple structure parallel to the polarisation direction of the pump beam was generated for pump powers of 5 and 12 mW. The spacing between microgrooves is not dependent on the power and polarisation direction of the pump beam, but the depth of the ripple structure increases if the power pump is increased. Due to the dichroism of the MR molecules, the depth is greater in the case of an Ar^+ laser beam polarised parallel to the rubbing direction. The azimuthal anchoring energy induced by the formed ripple structure can induce a surface-assisted photo-alignment effect. Our study demonstrates the possibility of controlling the orientation and depth of the ripple structure and, consequently, the induced anchoring energy by a proper choice of both power and polarisation direction of the pump beam.

Acknowledgement

The authors acknowledge Professor Anca-Luiza Alexe-Ionescu for fruitful discussions.

References

[1] Chigrinov, V.G.; Kozenkov, V.H.; Kwok, H.S. *Photoalignment of Liquid Crystalline Materials: Physics and Applications*; Wiley: New York, 2008.
[2] Lucchetti, L; Gentili, M.; Simoni, F. *Opt. Express* **2006**, *14*, 2236–2241.
[3] Fuh, A.Y.G.; Liao, C.C.; Hsu, K.C.; Lu, C.L.; Mo, T.S. *J. Nonlinear Opt. Phys. Mater*. **2002**, *11*, 57–63.
[4] Simoni, F.; Francescangeli, O. *J. Phys.: Condens. Matter* **1999**, *11*, R439–R487.
[5] Lee, C.R.; Fu, T.L.; Cheng, K.T.; Mo, T.S.; Fuh, A.Y.G. *Phys. Rev. E* **2004**, *69*, 031704.
[6] Fuh, A.Y.G.; Cheng, K.T.; Lee, C.R. *Jpn. J. Appl. Phys.* **2006**, *45*, 7024–7027.
[7] Huang, C.Y.; Lin, Y.R.; Lo, K.Y.; Lee, C.R. *Appl. Phys. Lett*. **2008**, *93*, 181114.
[8] Voloshchenko, D.; Khyzhnyak, A.; Reznikov, Y.; Reshtnyak, V. *Jpn. J. Appl. Phys*. **1995**, *34*, 566–571.
[9] Urbach, W; Hervet, H.; Rondelez, F. *J. Chem. Phys*. **1985**, *83*, 1877–1887.
[10] Sipe, J.E.; Yound, J.E.; Preston, J.S.; Van Driel, H.M. *Phys. Rev. B* **1983**, *27*, 1141–1154.
[11] Morita, S.; Wiesendanger, R.; Meyer, E. *Noncontact Atomic Force Microscopy*; Springer-Verlag: Heidelberg, 2002.
[12] Berreman, D.W. *Phys. Rev. Lett*. **1972**, *28*, 1683–1686.
[13] Sugimura, A.; Miyamoto, T.; Tsuji, M.; Kuze, M. *Appl. Phys. Lett.* **1998**, *72*, 329–331.